Hindawi Publishing Corporation
Mathematical Problems in Engineering
Volume 2010, Article ID 579162, 20 pages
doi:10.1155/2010/579162

Research Article

Effects of Slip and Heat Generation/Absorption on MHD Mixed Convection Flow of a Micropolar Fluid over a Heated Stretching Surface

Mostafa Mahmoud and Shimaa Waheed

Department of Mathematics, Faculty of Science, Benha University, Qalyubia 13518, Egypt

Correspondence should be addressed to Shimaa Waheed, shimaa_ezat@yahoo.com

Received 27 April 2010; Revised 20 June 2010; Accepted 21 July 2010

Academic Editor: Cristian Toma

A theoretical analysis is performed to study the flow and heat transfer characteristics of magnetohydrodynamic mixed convection flow of a micropolar fluid past a stretching surface with slip velocity at the surface and heat generation (absorption). The transformed equations solved numerically using the Chebyshev spectral method. Numerical results for the velocity, the angular velocity, and the temperature for various values of different parameters are illustrated graphically. Also, the effects of various parameters on the local skin-friction coefficient and the local Nusselt number are given in tabular form and discussed. The results show that the mixed convection parameter has the effect of enhancing both the velocity and the local Nusselt number and suppressing both the local skin-friction coefficient and the temperature. It is found that local skin-friction coefficient increases while the local Nusselt number decreases as the magnetic parameter increases. The results show also that increasing the heat generation parameter leads to a rise in both the velocity and the temperature and a fall in the local skin-friction coefficient and the local Nusselt number. Furthermore, it is shown that the local skin-friction coefficient and the local Nusselt number decrease when the slip parameter increases.

1. Introduction

Micropolar fluids are those with microstructure belonging to a class of complex fluids with nonsymmetrical stress tensor, and usually referred to as micromorphic fluids. Physically they represent fluids consisting of randomly oriented particles suspended in a viscous medium. The theory of micropolar fluid was first introduced and formulated by Eringen [1]. Later Eringen [2] generalized the theory to incorporate thermal effects in the so-called thermo-micropolar fluid. The theory of micropolar fluids is expected to provide a mathematical model for the non-Newtonian behavior observed in certain fluids such as liquid crystal [3, 4], low-concentration suspension flow [5, 6], blood rheology [7–10], the presence of dust or smoke [11, 12], and the effect of dirt in journal bearing [13–16].

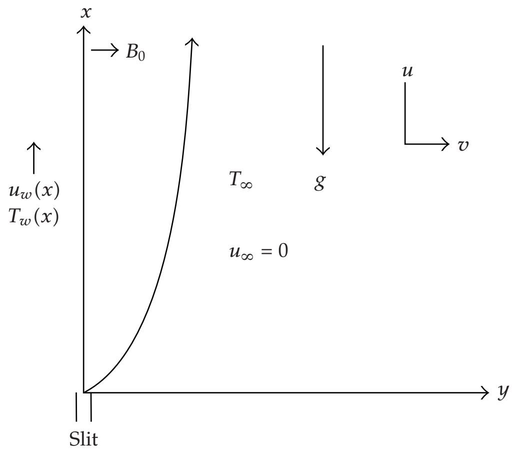

Figure 1: Coordinate system for the physical model.

On the other hand, flow of the fluids with microstructure due to a stretching surface and by thermal buoyancy is of considerable interest in several applications such as liquid crystal, dilute solutions of polymer fluids, and suspensions. Free and mixed convections of a micropolar fluid over a moving surface have been studied by many authors [17–25] under different situations.

In the above-mentioned studies, the effect of slip condition has not been taken into consideration, while fluids such as polymer melts often exhibit wall slip. Navier [26] proposed a slip boundary condition where the slip velocity depends linearly on the shear stress. Since then the effects of slip velocity on the boundary layer flow of non-Newtonian fluids have been studied by several authors [27–31]. The aim of this work is to investigate the effect of wall slip velocity on the flow and heat transfer of a micropolar fluid over a vertical stretching surface in the presence of heat generation (absorption) and magnetic field, where numerical solutions are obtained using Chebyshev spectral method. In our knowledge, this study was not investigated before despite many applications in polymer processing technology could be expected. For example, in the extrusion of polymer sheet from a die, the sheet is sometimes stretched. During this process, the properties of the final product depend considerably on the rate of cooling. By drawing such sheet in an electrically conducting fluid subjected to a magnetic field, the rate of cooling can be controlled and the final product can be obtained with desired characteristics. Also, the polymer processing involving exothermic chemical reaction and the working fluid heat generation effects are important. However, polymer melts often exhibit macroscopic wall slip.

2. Formulation of the Problem

Consider a steady, two-dimensional hydromagnetic laminar convective flow of an incompressible, viscous, micropolar fluid with a heat generation (absorption) on a stretching vertical surface with a velocity $u_w(x)$. The flow is assumed to be in the x-direction, which is taken along the vertical surface in upward direction and y-axis normal to it. A uniform magnetic field of strength B_0 is imposed along y-axis. The magnetic Reynolds number of the flow is taken to be small enough so that the induced magnetic field is assumed to be negligible. The gravitational acceleration g acts in the downward direction. The physical model and coordinate system are shown in Figure 1.

The temperature of the micropolar fluid far away from the plate is T_∞, whereas the surface temperature of the plate is maintained at T_w, where $T_w(x) = T_\infty + ax$, $a > 0$ is constant, and $T_w > T_\infty$. The temperature difference between the body surface and the surrounding micropolar fluid generates a buoyancy force, which results in an upward convective flow. Under usual boundary layer and Boussinesq approximations, the flow and heat transfer in the presence of heat generation (absorption) [32–35] are governed by the following equations:

$$\frac{\partial u}{\partial x} + \frac{\partial v}{\partial y} = 0, \tag{2.1}$$

$$u\frac{\partial u}{\partial x} + v\frac{\partial u}{\partial y} = \left(\nu + \frac{k}{\rho}\right)\frac{\partial^2 u}{\partial y^2} + \frac{k}{\rho}\frac{\partial N}{\partial y} + g\beta(T - T_\infty) - \frac{\sigma B_0^2}{\rho}u, \tag{2.2}$$

$$u\frac{\partial N}{\partial x} + v\frac{\partial N}{\partial y} = \frac{\gamma_0}{\rho j}\frac{\partial^2 N}{\partial y^2} - \frac{k}{\rho j}\left(2N + \frac{\partial u}{\partial y}\right), \tag{2.3}$$

$$u\frac{\partial T}{\partial x} + v\frac{\partial T}{\partial y} = \frac{\kappa}{\rho c_p}\frac{\partial^2 T}{\partial y^2} + \frac{Q_0}{\rho c_p}(T - T_\infty), \tag{2.4}$$

subject to the boundary conditions:

$$\begin{gathered} u = u_w(x) = cx + \alpha^*\left[(\mu + k)\frac{\partial u}{\partial y} + kN\right], \\ v = 0, \quad N = -m_0\frac{\partial u}{\partial y}, \quad T = T_w(x), \quad \text{at } y = 0, \\ u \longrightarrow 0, \quad N \to 0, \quad T \to T_\infty, \quad \text{as} y \longrightarrow \infty, \end{gathered} \tag{2.5}$$

where u and v are the velocity components in the x and y directions, respectively. T is the fluid temperature, N is the component of the microrotation vector normal to the x-y plane, ρ is the density, j is the microinertia density, μ is the dynamic viscosity, k is the gyro-viscosity (or vortex viscosity), β is the thermal expansion coefficient, σ is the electrical conductivity, c_p is the specific heat at constant pressure, κ is the thermal conductivity, c is a positive constant of proportionality, α^* is the slip coefficient, x measures the distance from the leading edge along the surface of the plate, and γ_0 is the spin-gradient viscosity.

We follow the recent work of the authors [36, 37] by assuming that γ_0 is given by

$$\gamma_0 = \left(\mu + \frac{k}{2}\right)j = \mu\left(1 + \frac{K}{2}\right)j. \tag{2.6}$$

This equation gives a relation between the coefficient of viscosity and microinertia, where $K = k/\mu(> 0)$ is the material parameter, $j = \nu/c$, $\sqrt{j}$ is the reference length, and m_0 $(0 \le m_0 \le 1)$ is the boundary parameter. When the boundary parameter $m_0 = 0$, we obtain $N = 0$ which is the no-spin condition, that is, the microelements in a concentrated particle flow close to the wall are not able to rotate (as stipulated by Jena and Mathur [38]). The case $m_0 = 1/2$ represents the weak concentration of microelements. The case corresponding to $m_0 = 1$ is used for the modelling of turbulent boundary layer flow (see Peddieson and Mcnitt [39]).

We introduce the following dimensionless variables:

$$\eta = \left(\frac{c}{\nu}\right)^{1/2} y, \qquad N = cx\left(\frac{c}{\nu}\right)^{1/2} g(\eta),$$
$$u = cxf'(\eta), \qquad v = -(c\nu)^{1/2} f, \tag{2.7}$$
$$\theta(\eta) = \frac{T - T_\infty}{T_w - T_\infty}.$$

Through (2.7), the continuity (2.1) is automatically satisfied and (2.2)–(2.4) will give then

$$(1+K)f''' + ff'' - f'^2 + Kg' - Mf' + \lambda\theta = 0, \tag{2.8}$$

$$\left(1 + \frac{K}{2}\right)g'' + fg' - f'g - K(2g + f'') = 0, \tag{2.9}$$

$$\frac{1}{\mathrm{Pr}}\theta'' + f\theta' - f'\theta + \gamma\theta = 0. \tag{2.10}$$

The transformed boundary conditions are then given by

$$f' = 1 + \alpha[1 + K(1 - m_0)]f'',$$
$$f = 0, \quad g = -m_0 f'', \quad \theta = 1, \quad \text{at } \eta = 0, \tag{2.11}$$
$$f' \to 0, \quad g \to 0, \quad \theta \to 0, \quad \text{as } \eta \to \infty,$$

where primes denote differentiation with respect to η, $M = \sigma B_0^2/c\rho$ is the magnetic parameter, $\lambda = g\beta a/c^2 (\geq 0)$ is the buoyancy parameter, $\alpha = \alpha^* \mu\sqrt{c/\nu}$ is the slip parameter, $\mathrm{Pr} = \mu c_p/\kappa$ is the Prandtl number, and $\gamma = Q_0/\rho c c_p$ is the heat generation (> 0) or absorption (< 0) parameter.

The physical quantities of interest are the local skin-friction coefficient C_{f_x} and the local Nusselt number N_{u_x}, which are defined, respectively, as,

$$C_{f_x} = \frac{2\tau_w}{\rho(cx)^2},$$
$$Nu_x = \frac{xq_w}{\kappa(T_w - T_\infty)}, \tag{2.12}$$

where the wall shear stress τ_w and the heat transfer from the plate q_w are defined by

$$\tau_w = -\left[(\mu + k)\frac{\partial u}{\partial y} + kN\right]_{y=0},$$
$$q_w = -\left[\kappa\frac{\partial T}{\partial y}\right]_{y=0}. \tag{2.13}$$

Using (2.7), we get

$$\frac{1}{2}C_{f_x}\mathrm{Re}_x^{1/2} = -(1+K(1-m_0))f''(0), \quad Nu_x\mathrm{Re}_x^{-1/2} = -\theta'(0), \tag{2.14}$$

where $\mathrm{Re}_x = (cx^2/\nu)$ is the local Reynolds number.

3. Method of Solution

The domain of the governing boundary layer equations (2.8)–(2.10) is the unbounded region $[0,\infty)$. However, for all practical reasons, this could be replaced by the interval $0 \le \eta \le \eta_\infty$, where η_∞ is some large number to be specified for computational convenience. Using the following algebraic mapping:

$$\chi = 2\frac{\eta}{\eta_\infty} - 1, \tag{3.1}$$

the unbounded region $[0,\infty)$ is finally mapped onto the finite domain $[-1,1]$, and the problem expressed by (2.8)–(2.10) is transformed into

$$\begin{gathered}(1+K)f'''(\chi)+\left(\frac{\eta_\infty}{2}\right)\left(f(\chi)f''(\chi)-f'^2(\chi)\right)+\left(\frac{\eta_\infty}{2}\right)^2(Kg'(\chi)-Mf'(\chi))+\lambda\left(\frac{\eta_\infty}{2}\right)^3\theta(\chi)=0,\\ \left(1+\frac{K}{2}\right)g''(\chi)+\left(\frac{\eta_\infty}{2}\right)(f(\chi)g'(\chi)-g(\chi)f'(\chi))-K\left(2\left(\frac{\eta_\infty}{2}\right)^2g(\chi)+f''(\chi)\right)=0,\\ \frac{1}{\mathrm{Pr}}\theta''(\chi)+\left(\frac{\eta_\infty}{2}\right)(f(\chi)\theta'(\chi)-f'(\chi)\theta(\chi))+\left(\frac{\eta_\infty}{2}\right)^2\gamma\theta(\chi)=0.\end{gathered} \tag{3.2}$$

The transformed boundary conditions are given by

$$\begin{gathered}f(-1)=0,\quad f'(-1)=\left(\frac{\eta_\infty}{2}\right)+\left(\frac{2}{\eta_\infty}\right)\alpha(1+K(1-m_0))f''(-1),\quad f'(1)=0,\\ g(-1)=-m_0\left(\frac{2}{\eta_\infty}\right)^2f''(-1),\quad g(1)=0,\\ \theta(-1)=1,\quad \theta(1)=0.\end{gathered} \tag{3.3}$$

Our technique is accomplished by starting with a Chebyshev approximation for the highest order derivatives, f''', g'', and θ'' and generating approximations to the lower-order derivatives f'', f', f, g', g, θ', and θ as follows.

Setting $f''' = \phi(\chi)$, $g'' = \psi(\chi)$ and $\theta'' = \zeta(\chi)$, then by integration we obtain

$$\begin{aligned}
f''(\chi) &= \int_{-1}^{\chi} \phi(\chi)d\chi + C_1^f, \\
f'(\chi) &= \iint_{-1}^{\chi} \phi(\chi)d\chi\, d\chi + C_1^f(\chi+1) + C_2^f, \\
f(\chi) &= \iiint_{-1}^{\chi} \phi(\chi)d\chi\, d\chi\, d\chi + C_1^f \frac{(\chi+1)^2}{2} + C_2^f(\chi+1) + C_3^f, \\
g'(\chi) &= \int_{-1}^{\chi} \psi(\chi)d\chi + C_1^g, \\
g(\chi) &= \iint_{-1}^{\chi} \psi(\chi)d\chi\, d\chi + C_1^g(\chi+1) + C_2^g, \\
\theta'(\chi) &= \int_{-1}^{\chi} \zeta(\chi)d\chi + C_1^\theta, \\
\theta(\chi) &= \iint_{-1}^{\chi} \zeta(\chi)d\chi\, d\chi + C_1^\theta(\chi+1) + C_2^\theta.
\end{aligned} \tag{3.4}$$

From the boundary condition (3.3), we obtain

$$\begin{gathered}
C_1^f = -\frac{1}{2+\alpha(1+K(1-m_0))(2/\eta_\infty)} \int_{-1}^{1}\int_{-1}^{\chi} \phi(\chi)d\chi\, d\chi - \frac{1}{2+\alpha(1+K(1-m_0))(2/\eta_\infty)} \left(\frac{\eta_\infty}{2}\right), \\
C_2^f = \left(\frac{\eta_\infty}{2}\right) + \alpha(1+K(1-m_0))\left(\frac{2}{\eta_\infty}\right)C_1^f, \\
C_3^f = 0, \\
C_1^g = -\frac{1}{2}\int_{-1}^{1}\int_{-1}^{\chi} \psi(\chi)d\chi - \frac{1}{2}C_2^g, \\
C_2^g = -\frac{m_0(2/\eta_\infty)^2}{2+\alpha(1+K(1-m_0))(2/\eta_\infty)} \int_{-1}^{1}\int_{-1}^{\chi} \phi(\chi)d\chi\, d\chi + \frac{m_0(2/\eta_\infty)}{2+\alpha(1+K(1-m_0))(2/\eta_\infty)}, \\
C_1^\theta = -\frac{1}{2}\int_{-1}^{1}\int_{-1}^{\chi} \zeta(\chi)d\chi d\chi - \frac{1}{2}, \\
C_2^\theta = 1.
\end{gathered} \tag{3.5}$$

Therefore, we can give approximations to (3.4) as follows:

$$
\begin{gathered}
f_i(\chi)=\sum_{j=0}^{N} l_{ij}^{f}\phi_j+d_i^{f},\quad f_i'(\chi)=\sum_{j=0}^{N} l_{ij}^{f1}\phi_j+d_i^{f1},\quad f_i''(\chi)=\sum_{j=0}^{N} l_{ij}^{f2}\phi_j+d_i^{f2},\\
g_i(\chi)=\sum_{j=0}^{N} l_{ij}^{\theta}\psi_j+\sum_{j=0}^{N} l_{ij}^{g}\phi_j+d_i^{g},\quad g_i'(\chi)=\sum_{j=0}^{N} l_{ij}^{\theta 1}\psi_j+\sum_{j=0}^{N} l_{ij}^{g1}\phi_j+d_i^{g1},\\
\theta_i(\chi)=\sum_{j=0}^{N} l_{ij}^{\theta}\zeta_j+d_i^{\theta},\quad \theta_i'(\chi)=\sum_{j=0}^{N} l_{ij}^{\theta 1}\zeta_j+d_i^{\theta 1},
\end{gathered}
\tag{3.6}
$$

for all $i=0(1)N$, where

$$
\begin{aligned}
l_{ij}^{\theta}&=b_{ij}^{2}-\frac{(\chi_i+1)}{2}b_{Nj}^{2},\quad d_i^{\theta}=1-\frac{(\chi_i+1)}{2},\\
l_{ij}^{\theta 1}&=b_{ij}-\frac{1}{2}b_{Nj}^{2},\quad d_i^{\theta 1}=-\frac{1}{2},\\
l_{ij}^{g}&=\frac{m_0(2/\eta_\infty)^2}{2+\alpha(1+K(1-m_0))(2/\eta_\infty)}\left(1-\frac{(\chi_i+1)}{2}\right)b_{Nj}^{2},\\
d_i^{g}&=\frac{m_0(2/\eta_\infty)}{2+\alpha(1+K(1-m_0))(2/\eta_\infty)}\left(1-\frac{(\chi_i+1)}{2}\right),\\
l_{ij}^{g1}&=-\frac{m_0(2/\eta_\infty)^2}{2(2+\alpha(1+K(1-m_0))(2/\eta_\infty))}b_{Nj}^{2},\\
d_i^{g1}&=-\frac{m_0(2/\eta_\infty)}{2(2+\alpha(1+K(1-m_0))(2/\eta_\infty))},\\
l_{ij}^{f}&=b_{ij}^{3}-\frac{1}{2+\alpha(1+K(1-m_0))(2/\eta_\infty)}\left[\frac{(\chi_i+1)^2}{2}+\alpha(1+K(1-m_0))(\chi_i+1)\left(\frac{2}{\eta_\infty}\right)\right]b_{Nj}^{2},\\
d_i^{f}&=(\chi_i+1)\left(\frac{\eta_\infty}{2}\right)-\frac{(\eta_\infty/2)}{2+\alpha(1+K(1-m_0))(2/\eta_\infty)}\\
&\quad\times\left[\frac{(\chi_i+1)^2}{2}+\alpha(1+K(1-m_0))(\chi_i+1)\left(\frac{2}{\eta_\infty}\right)\right],\\
l_{ij}^{f1}&=b_{ij}^{2}-\frac{1}{2+\alpha(1+K(1-m_0))(2/\eta_\infty)}\left[(\chi_i+1)+\alpha(1+K(1-m_0))\left(\frac{2}{\eta_\infty}\right)\right]b_{Nj}^{2},\\
d_i^{f1}&=\left(\frac{\eta_\infty}{2}\right)-\frac{(\eta_\infty/2)}{2+\alpha(1+K(1-m_0))(2/\eta_\infty)}\left[(\chi_i+1)+\alpha(1+K(1-m_0))\left(\frac{2}{\eta_\infty}\right)\right],
\end{aligned}
$$

$$
\begin{aligned}
l_{ij}^{f2} &= b_{ij} - \frac{1}{2+\alpha(1+K(1-m_0))(2/\eta_\infty)} b_{Nj}^2, \\
d_i^{f2} &= -\frac{(\eta_\infty/2)}{2+\alpha(1+K(1-m_0))(2/\eta_\infty)},
\end{aligned}
\tag{3.7}
$$

where

$$
b_{ij}^2 = (\chi_i - \chi_j) b_{ij}, \quad i = 0(1)N, \tag{3.8}
$$

and b_{ij} are the elements of the matrix B, as given in [40, 41].

By using (3.6), one can transform (3.2) to the following system of nonlinear equations in the highest derivatives:

$$
\begin{aligned}
&(1+K)\phi_i + \left(\frac{\eta_\infty}{2}\right)\left[\left(\sum_{j=0}^{N} l_{ij}^{f}\phi_j + d_i^{f}\right)\left(\sum_{j=0}^{N} l_{ij}^{f2}\phi_j + d_i^{f2}\right) - \left(\sum_{j=0}^{N} l_{ij}^{f1}\phi_j + d_i^{f1}\right)^2\right] \\
&\quad + \left(\frac{\eta_\infty}{2}\right)^2\left[K\left(\sum_{j=0}^{N} l_{ij}^{\theta 1}\varphi_j + \sum_{j=0}^{N} l_{ij}^{g1}\phi_j + d_i^{g1}\right) - M\left(\sum_{j=0}^{N} l_{ij}^{f1}\phi_j + d_i^{f1}\right)\right] \\
&\quad + \lambda\left(\frac{\eta_\infty}{2}\right)^3\left(\sum_{j=0}^{N} l_{ij}^{\theta}\zeta_j + d_i^{\theta}\right) = 0, \\
&\left(1+\frac{K}{2}\right)\varphi_i + \left(\frac{\eta_\infty}{2}\right)\left[\left(\sum_{j=0}^{N} l_{ij}^{f}\phi_j + d_i^{f}\right)\left(\sum_{j=0}^{N} l_{ij}^{\theta 1}\varphi_j + \sum_{j=0}^{N} l_{ij}^{g1}\phi_j + d_i^{g1}\right)\right. \\
&\qquad\qquad \left. - \left(\sum_{j=0}^{N} l_{ij}^{\theta}\varphi_j + \sum_{j=0}^{N} l_{ij}^{g}\phi_j + d_i^{g}\right)\left(\sum_{j=0}^{N} l_{ij}^{f1}\phi_j + d_i^{f1}\right)\right] \\
&\quad - K\left(2\left(\frac{\eta_\infty}{2}\right)^2\left(\sum_{j=0}^{N} l_{ij}^{\theta}\varphi_j + \sum_{j=0}^{N} l_{ij}^{g}\phi_j + d_i^{g}\right) + \left(\sum_{j=0}^{N} l_{ij}^{f2}\phi_j + d_i^{f2}\right)\right) = 0, \\
&\frac{1}{\Pr}\zeta_i + \left(\frac{\eta_\infty}{2}\right)\left[\left(\sum_{j=0}^{N} l_{ij}^{f}\phi_j + d_i^{f}\right)\left(\sum_{j=0}^{N} l_{ij}^{\theta 1}\zeta_j + d_i^{\theta 1}\right) - \left(\sum_{j=0}^{N} l_{ij}^{f1}\phi_j + d_i^{f1}\right)\left(\sum_{j=0}^{N} l_{ij}^{\theta}\zeta_j + d_i^{\theta}\right)\right] \\
&\quad + \left(\frac{\eta_\infty}{2}\right)^2\gamma\left(\sum_{j=0}^{N} l_{ij}^{\theta}\zeta_j + d_i^{\theta}\right) = 0.
\end{aligned}
\tag{3.9}
$$

This system is solved using Newton's iteration.

Table 1: Comparison of $(1/2)\, C_{f_x}\, \mathrm{Re}_x^{1/2}$ for various values of m_0 and K with $M = 0$, $\alpha = 0$, and $\lambda = 0$.

m_0	0		1/2	
K	Nazar et al. [42]	Present work	Nazar et al. [42]	Present work
0	−1.0000	−1.00001	−1.0000	−1.00001
1	−1.3679	−1.36799	−1.2247	−1.22482
2	−1.6213	−1.62150	−1.4142	−1.41440
4	−2.0042	−2.00452	−1.7321	−1.73291

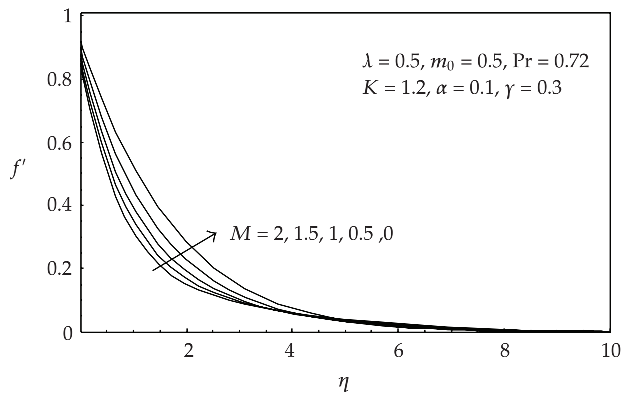

Figure 2: Velocity profiles for various values of M.

4. Results and Discussion

To verify the proper treatment of the problem, our numerical results have been compared for local skin-friction coefficient $(1/2)C_{f_x}\mathrm{Re}_x^{1/2}$ taking $M = 0$ and $\lambda = 0$ in (2.8) with those obtained by Nazar et al. [42] for various values of K and m_0. The results of this comparison are given in Table 1. Table 2 shows the comparison of our numerical results obtained for $-\theta'(0)$ taking $\gamma = 0$, $K = 0$, and $m_0 = 0$ (with constant wall temperatures) in (2.10) with those reported by Ishak [43], Grubka and Bobba [44], Ali [45] and Chen [46] for various values of Pr. The results show a good agreement.

To study the behavior of the velocity, the angular velocity, and the temperature profiles, curves are drawn in Figures 2–19. The effect of various parameters, namely, the magnetic parameter M, the material parameter K, the slip parameter α, the buoyancy parameter λ, the heat generation (absorption) parameter γ, and the Prandtl number Pr have been studied over these profiles.

Figures 2–4 illustrate the variation of the velocity f', the angular velocity g, and the temperature θ profiles with the magnetic parameter M. Figure 2 depicts the variation of f' with M. It is observed that f' decreases with the increase in M along the surface. This indicates that the fluid velocity is reduced by increasing the magnetic field and confines the fact that application of a magnetic field to an electrically conducting fluid produces a drag-like force which causes reduction in the fluid velocity. The profile of the angular velocity g with the variation of M is shown in Figure 3. It is clear from this figure that g increases with an increase in M near the surface and the reverse is true away from the surface. Figure 4

Table 2: Comparison of $-\theta'(0)$ for various values of Pr with $\gamma = K = \lambda = M = 0$, $\alpha = 0$, and $m_0 = 0.5$.

Pr	Grubka and Bobba [44]	Ali [45]	Chen [46]	Ishak [43]	Present work
0.72	0.4631	0.4617	0.46315	0.4631	0.46315
1.0	0.5820	0.5801	0.58199	0.5820	0.58201
3.0	1.1652	1.1599	1.16523	1.1652	1.16507
10	2.3080	2.2960	2.30796	2.3080	2.29645
100	7.7657	—	7.76536	7.7657	7.76782

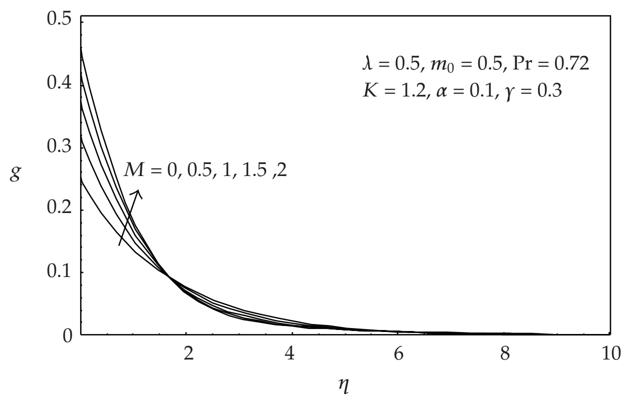

Figure 3: Angular velocity profiles for various values of M.

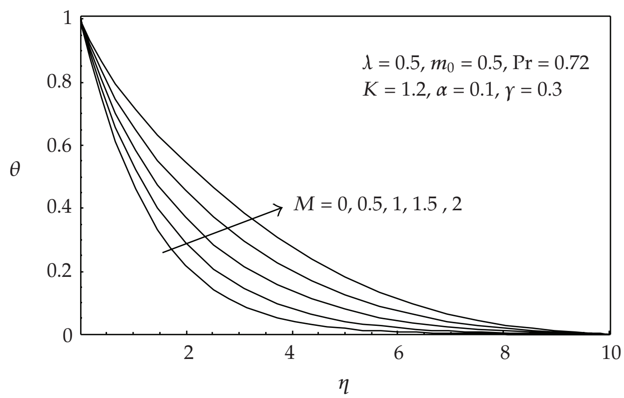

Figure 4: Temperature profiles for various values of M.

shows the resulting temperature profile θ for various values of M. It is noted that an increase of M leads to an increase of θ.

Figure 5 illustrates the effects of the material parameter K on f'. It can be seen from this figure that the velocity decreases as the material parameter K rises near the surface and the opposite is true away from it. Also, it is noticed that the material parameter has no effect on the boundary layer thickness. The effect of K on g is shown in Figure 6. It is observed that initially g decreases by increasing K near the surface and the reverse is true away from the surface. Figure 7 demonstrates the variation of θ with K. From this figure it is clear that θ decreases with an increase in K.

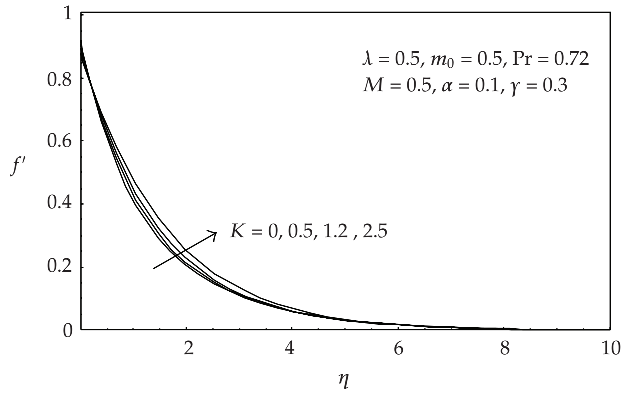

Figure 5: Velocity profiles for various values of K.

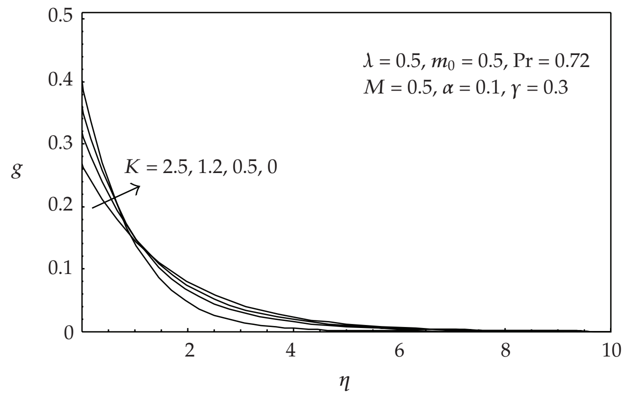

Figure 6: Angular velocity profiles for various values of K.

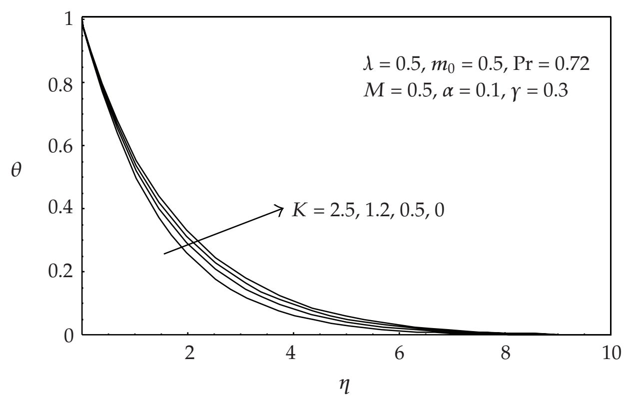

Figure 7: Temperature profiles for various values of K.

Figures 8, 9, and 10 depict the effect of the slip parameter on f', g, and θ, respectively. It is seen that f' and g decrease as α increases, near the surface and they increase at larger distance from the surface, while θ increases as α increases in the boundary layer region.

It was observed from Figure 11 that the velocity increases for large values of λ while the boundary layer thickness is the same for all values of λ. Figure 12 depicts the effects of λ

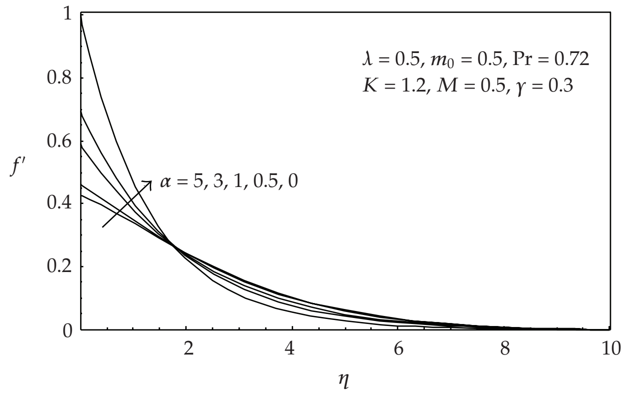

Figure 8: Velocity profiles for various values of α.

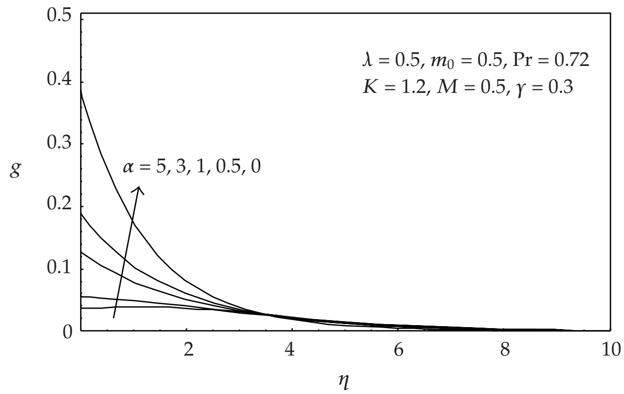

Figure 9: Angular velocity profiles for various values of α.

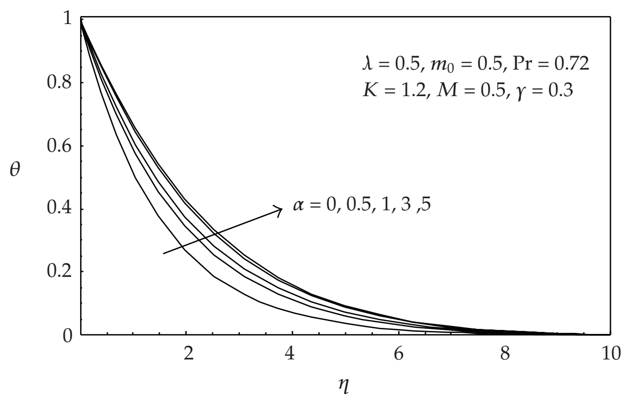

Figure 10: Temperature profiles for various values of α.

on g. The angular velocity g is a decreasing function of λ near the surface and the reverse is true at larger distance from the surface. Figure 13 shows the variations of λ on θ. It is found that θ decreases with an increase in λ.

Figure 14 shows the effect of the heat generation parameter ($\gamma > 0$) or the heat absorption parameter ($\gamma < 0$) on f'. It is observed that f' increases as the heat generation

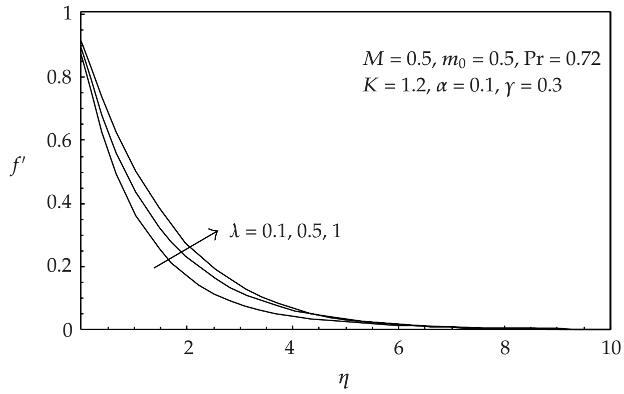

Figure 11: Velocity profiles for various values of λ.

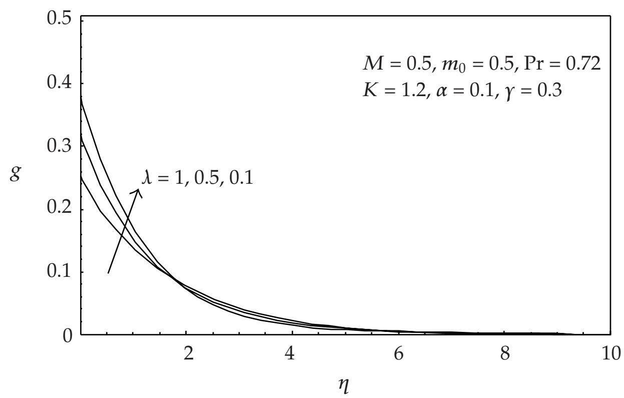

Figure 12: Angular velocity profiles for various values of λ.

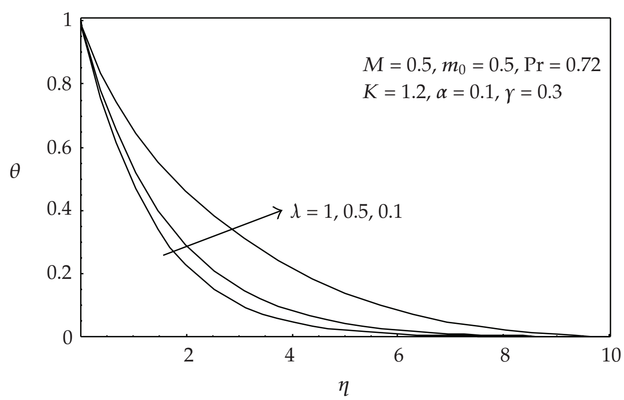

Figure 13: Temperature profiles for various values of λ.

parameter ($\gamma > 0$) increases, but the effect of the absolute value of heat absorption parameter ($\gamma < 0$) is the opposite. The effect of the heat generation parameter ($\gamma > 0$) or the heat absorption parameter ($\gamma < 0$) on g within the boundary layer region is observed in Figure 15.

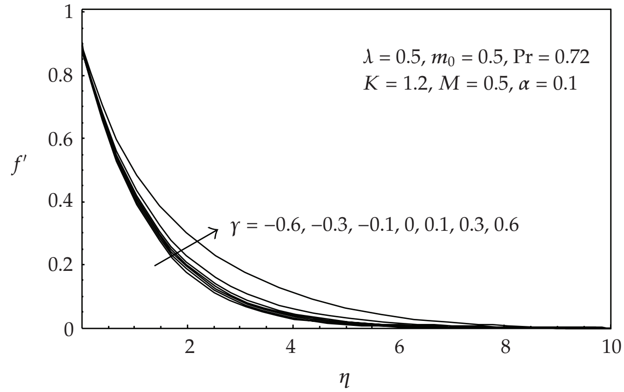

Figure 14: Velocity profiles for various values of γ.

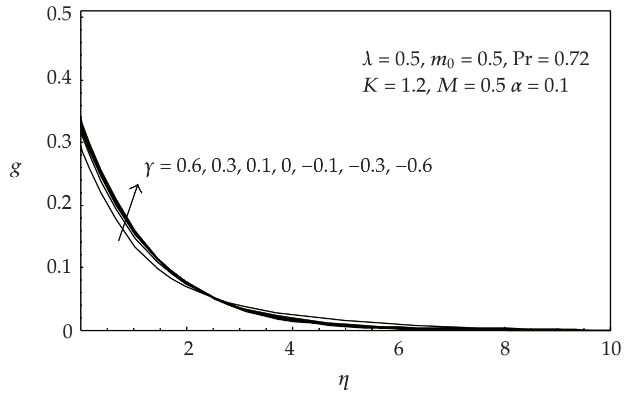

Figure 15: Angular velocity profiles for various values of γ.

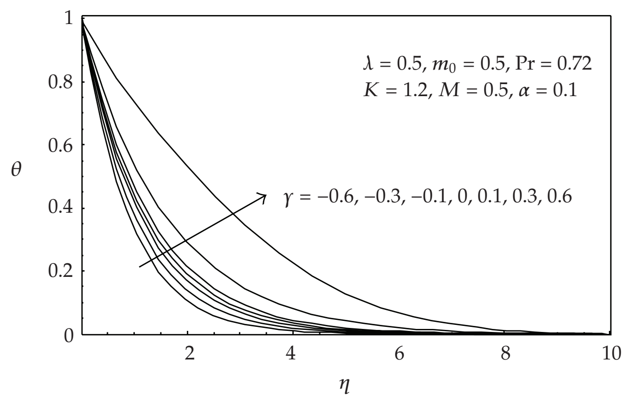

Figure 16: Temperature profiles for various values of γ.

It is apparent from this figure that g increases as the heat generation parameter ($\gamma > 0$) decreases, while g increases as the absolute value of heat absorption parameter ($\gamma < 0$) increases near the surface and the reverse is true away from the surface. Figure 16 displays the effect of the heat generation parameter ($\gamma > 0$) or the heat absorption parameter ($\gamma < 0$) on θ.

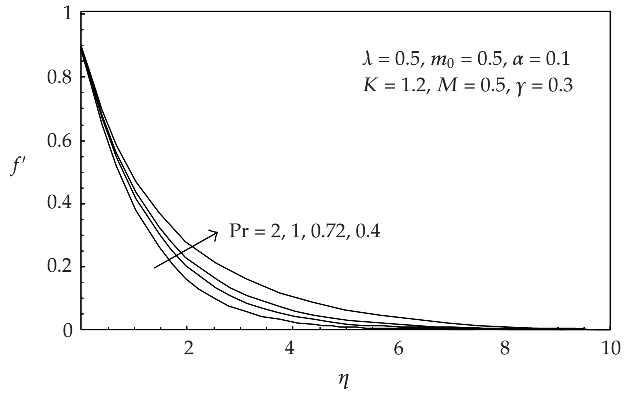

Figure 17: Velocity profiles for various values of Pr.

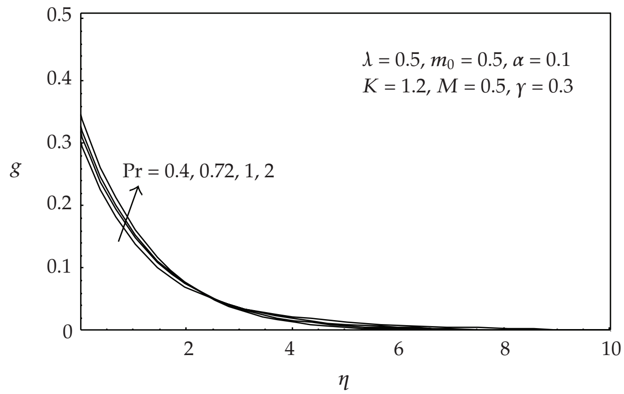

Figure 18: Angular velocity profiles for various values ofPr.

It is shown that as the heat generation parameter ($\gamma > 0$) increases, the thermal boundary layer thickness increases. For the case of the absolute value of the heat absorption parameter ($\gamma < 0$), one sees that the thermal boundary layer thickness decreases as γ increases.

The effect of the Prandtl number Pr on the velocity, the angular velocity, and the temperature profiles is illustrated in Figures 17, 18, and 19. From these figures, it can be seen that f' decrease with increasing Pr, while g increases as the Prandtl number Pr increases near the surface and the reverse is true away from the surface. The temperature θ of the fluid decreases with an increase of the Prandtel number Pr as shown in Figure 19. This is in agreement with the fact that the thermal boundary layer thickness decreases with increasing Pr. Figure 20 presented the local skin-friction coefficient and the local Nusselt number for different values of λ and K keeping all other parameters fixed. It is noticed that as K increases, the local skin-friction coefficient as well as the local Nusselt number increase considerably for a fixed value of λ. Also, it is observed that for a fixed value of K the local skin-friction coefficient decreases, while the local Nusselt number increases as λ increases. The variation of the local skin-friction coefficient and the local Nusselt number with λ for various of Pr when all other parameters fixed are shown in Figure 21. It is found that both the local skin-friction coefficient and the local Nusselt number increase with increasing Pr for a fixed value

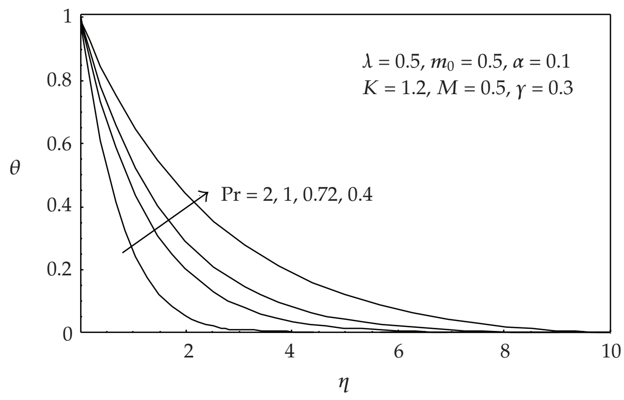

Figure 19: Temperature profiles for various values of Pr.

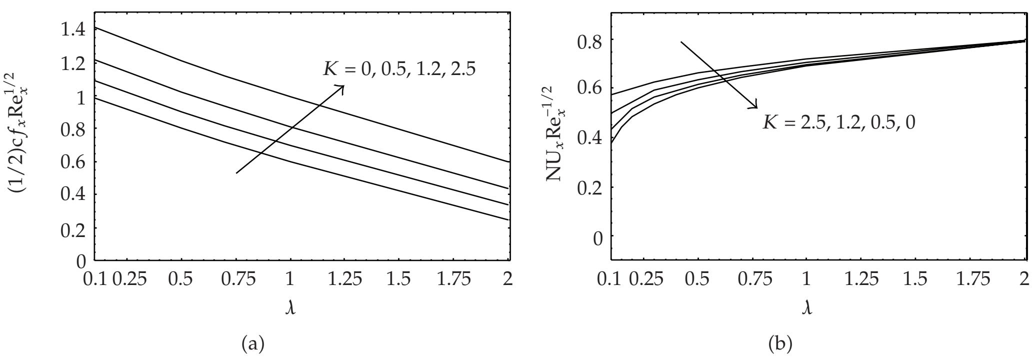

Figure 20: (a) Local skin Friction coefficient as a function of λ for various values of K when Pr = 0.72, $\alpha = 0.1$, $\gamma = 0.3$, and M = 0.5; (b) Local Nusselt number as a function of λ for various values of K when Pr = 0.72, $\alpha = 0.1$, $\gamma = 0.3$, and M = 0.5.

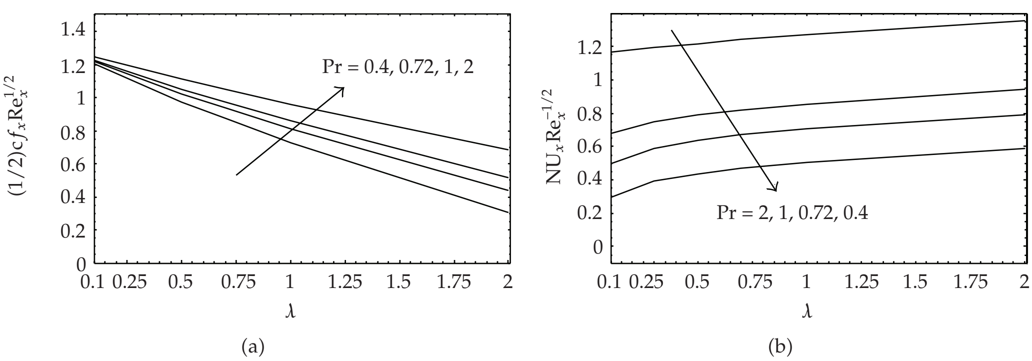

Figure 21: (a) Local skin Friction coefficient as a function of λ for various values of Pr when K = 1.2, $\alpha = 0.1$, $\gamma = 0.3$, and M = 0.5. (b) Local Nusselt number as a function of λ for various values of Pr when K = 1.2, $\alpha = 0.1$, $\gamma = 0.3$, and M = 0.5.

Table 3: Values of $-f''(0)$, $-g(0)$, and $-\theta'(0)$ for various values of M, λ, α, and γ with $m_0 = 1/2$, K = 1.2, and Pr = 0.72.

M	λ	α	γ	$-f''(0)$	$-g(0)$	$-\theta'(0)$
0	0.5	0.1	0.3	0.504574	0.169694	0.715432
0.5	0.5	0.1	0.3	0.638351	0.238366	0.637005
1	0.5	0.1	0.3	0.747640	0.295908	0.560481
1.5	0.5	0.1	0.3	0.840622	0.345823	0.484358
2	0.5	0.1	0.3	0.921943	0.390125	0.408426
0.5	0.1	0.1	0.3	0.754938	0.296486	0.497523
0.5	0.5	0.1	0.3	0.638351	0.238366	0.637005
0.5	1	0.1	0.3	0.507318	0.168166	0.707658
0.5	1.5	0.1	0.3	0.387608	0.099562	0.755669
0.5	2	0.1	0.3	0.275305	0.032101	0.793617
0.5	0.5	0	0.3	0.775613	0.308053	0.685894
0.5	0.5	0.5	0.3	0.380863	0.118681	0.534004
0.5	0.5	1	0.3	0.255840	0.066494	0.477392
0.5	0.5	3	0.3	0.111754	0.011758	0.405266
0.5	0.5	5	0.3	0.071653	0.002299	0.383641
0.5	0.5	0.1	−0.6	0.680866	0.250162	1.069730
0.5	0.5	0.1	−0.3	0.672210	0.247389	0.953975
0.5	0.5	0.1	−0.1	0.664555	0.245108	0.865909
0.5	0.5	0.1	0	0.659817	0.243775	0.817112
0.5	0.5	0.1	0.1	0.654173	0.242260	0.763916
0.5	0.5	0.1	0.3	0.638351	0.238366	0.637005
0.5	0.5	0.1	0.6	0.591894	0.227559	0.339497

of λ. For a fixed Pr, the local skin-friction coefficient decreases, while the local Nusselt number increases as λ increases.

The local skin-friction coefficient in terms of $-f''(0)$ and the local Nusselt number in terms of $-\theta'(0)$ for various values of M, λ, α, and γ are tabulated in Table 3. It is obvious from this table that local skin-friction coefficient increases with the increase of the magnetic parameter M and the absolute values of the heat absorption parameter ($\gamma < 0$) while it decreased as the slip parameter α, the buoyancy parameter λ, and the heat generation parameter ($\gamma > 0$) increase. The local Nusselt number increases with the increase of the buoyancy parameter λ. It is found that an increase in the magnetic parameter M and the slip parameter α leads to a decrease in the local Nusselt number. Also, the local Nusselt number decreases with the increase of the heat generation parameter ($\gamma > 0$), while it increased with the increase of the absolute value of the heat absorption parameter ($\gamma < 0$).

5. Conclusions

In the present work, the effects of heat generation (absorption) and a transverse magnetic field on the flow and heat transfer of a micropolar fluid over a vertical stretching surface with surface slip have been studied. The governing fundamental equations are transformed to a system of nonlinear ordinary differential equations which is solved numerically. The velocity, the angular velocity, and the temperature fields as well as the local skin-friction coefficient and the local Nusselt number are presented for various values of the parameters governing the problem.

From the numerical results, we can observe that, the velocity decreases with increasing the magnetic parameter, and the absolute value of the heat absorption parameter, while it increases with increasing the buoyancy parameter, the heat generation parameter, and the Prandtl number. Also, it is found that near the surface the velocity decreases as the slip parameter and the material parameter increase, while the reverse happens as one moves away from the surface. The angular velocity decreases with increasing the material parameter, the slip parameter, the buoyancy parameter, and the heat generation parameter, while it increases with increasing the magnetic parameter, the absolute value of the heat absorption parameter, and the Prandtl number near the surface and the reverse is true away from the surface. In addition the temperature distribution increases with increasing the slip parameter, the heat generation parameter, and the magnetic parameter, but it decreases with increasing the Prandtl number, the buoyancy parameter, the material parameter, and the absolute value of the heat absorption parameter. Moreover, the local skin-friction coefficient increases with increasing the magnetic parameter and the absolute value of the heat absorption parameter, while the local skin-friction decreases with increasing the buoyancy parameter, the slip parameter, and the heat generation parameter. Finally, the local Nusselt number increases with increasing the buoyancy parameter, and the absolute value of the heat absorption parameter, and decreases with increasing the magnetic parameter, the slip parameter, and the heat generation parameter.

Acknowledgment

The authors are thankful to the reviewers for their constructive comments which improve the paper.

References

[1] A. C. Eringen, "Theory of micropolar fluids," *Journal of Mathematics and Mechanics*, vol. 16, pp. 1–18, 1966.
[2] A. C. Eringen, "Theory of thermo micropolar fluids," *Journal of Applied Mathematics*, vol. 38, pp. 480–495, 1972.
[3] J. D. Lee and A. C. Eringen, "Wave propagation in nematic liquid crystals," *The Journal of Chemical Physics*, vol. 54, no. 12, pp. 5027–5034, 1971.
[4] J. D. Lee and A. C. Eringen, "Boundary effects of orientation of nematic liquid crystals," *The Journal of Chemical Physics*, vol. 55, no. 9, pp. 4509–4512, 1971.
[5] T. Ariman, M. A. Turk, and N. D. Sylvester, "Applications of microcontinuum fluid mechanics," *International Journal of Engineering Science*, vol. 12, no. 4, pp. 273–293, 1974.
[6] T. Ariman, M. A. Turk, and N. D. Sylvester, "Microcontinuum fluid mechanics-a review," *International Journal of Engineering Science*, vol. 11, no. 8, pp. 905–915, 1973.
[7] K. A. Kline and S. J. Allen, "Pulsatile blood flow investigation of particle concentration effects," *Biorheology*, vol. 6, pp. 99–110, 1969.
[8] T. Ariman, "On the analysis of blood flow," *Journal of Biomechanics*, vol. 4, no. 3, pp. 185–192, 1971.
[9] T. Ariman, "Heat conduction in blood," in *Proceedings of the ASCE Engineering Mechanics Division Specialty Conference*, January 1971.
[10] J. C. Misra and K. Roychoudhury, "Non linear stress field in blood vessels under the actionof connective tissues," *Blood Vessels*, vol. 19, pp. 19–29, 1982.
[11] Y. Y. Lok, N. Amin, and I. Pop, "Unsteady mixed convection flow of a micropolar fluid near the stagnation point on a vertical surface," *International Journal of Thermal Sciences*, vol. 45, no. 12, pp. 1149–1157, 2006.

[12] K. Chandra, “Instability of fluids heated from below,” *Proceedings of the Royal Society A*, vol. 164, pp. 231–224, 1938.

[13] S. Allen and K. Kline, “Lubrication theory for micropolar fluids,” *Journal of Applied Mechanics*, vol. 38, pp. 646–656, 1971.

[14] M. M. Khonsari, “On the self-excited whirl orbits of a journal in a sleeve bearing lubricated with micropolar fluids,” *Acta Mechanica*, vol. 81, no. 3-4, pp. 235–244, 1990.

[15] J. Prakash and P. Sinha, “Lubrication theory for micropolar fluids and its application to a journal bearing,” *International Journal of Engineering Science*, vol. 13, no. 3, pp. 217–232, 1975.

[16] N. Tipei, “Lubrication with micropolar liquids and its application to short bearings,” *Journal of Lubrication Technology*, vol. 101, no. 3, pp. 356–363, 1979.

[17] Y. J. Kim and A. G. Fedorov, “Transient mixed radiative convection flow of a micropolar fluid past a moving, semi-infinite vertical porous plate,” *International Journal of Heat and Mass Transfer*, vol. 46, no. 10, pp. 1751–1758, 2003.

[18] R. Bhargava, L. Kumar, and H. S. Takhar, “Mixed convection from a continuous surface in a parallel moving stream of a micropolar fluid,” *Heat and Mass Transfer*, vol. 39, no. 5-6, pp. 407–413, 2003.

[19] M. M. Rahman and M. A. Sattar, “Transient convective flow of micropolar fluid past a continuously-moving vertical porous plate in the presence of radiation,” *International Journal of Applied Mechanics and Engineering*, vol. 12, pp. 497–513, 2007.

[20] M. M. Rahman and M. A. Sattar, “Magnetohydrodynamic convective flow of a micropolar fluid past a continuously moving vertical porous plate in the presence of heat generation/absorption,” *Journal of Heat Transfer*, vol. 128, no. 2, pp. 142–152, 2006.

[21] A. Ishak, R. Nazar, and I. Pop, “Heat transfer over a stretching surface with variable heat flux in micropolar fluids,” *Physics Letters A*, vol. 372, no. 5, pp. 559–561, 2008.

[22] A. Ishak, R. Nazar, and I. Pop, “Mixed convection stagnation point flow of a micropolar fluid towards a stretching sheet,” *Meccanica*, vol. 43, no. 4, pp. 411–418, 2008.

[23] A. Ishak, R. Nazar, and I. Pop, “Magnetohydrodynamic (MHD) flow of a micropolar fluid towards a stagnation point on a vertical surface,” *Computers and Mathematics with Applications*, vol. 56, no. 12, pp. 3188–3194, 2008.

[24] A. Ishak, Y. Y. Lok, and I. Pop, “Stagnation-point flow over a shrinking sheet in a micropolarfluid,” *Chemical Engineering Communications*, vol. 197, pp. 1417–1427, 2010.

[25] T. Hayat, Z. Abbas, and T. Javed, “Mixed convection flow of a micropolar fluid over a non-linearly stretching sheet,” *Physics Letters A*, vol. 372, no. 5, pp. 637–647, 2008.

[26] C. L. M. Navier, “Sur les lois du mouvement des fluides,” *Memoires de l'Academie Royale des Sciences*, vol. 6, pp. 389–440, 1827.

[27] P. D. Ariel, T. Hayat, and S. Asghar, “The flow of an elastico-viscous fluid past a stretching sheet with partial slip,” *Acta Mechanica*, vol. 187, no. 1–4, pp. 29–35, 2006.

[28] T. Hayat, T. Javed, and Z. Abbas, “Slip flow and heat transfer of a second grade fluid past a stretching sheet through a porous space,” *International Journal of Heat and Mass Transfer*, vol. 51, no. 17-18, pp. 4528–4534, 2008.

[29] T. Hayat, M. Khan, and M. Ayub, “The effect of the slip condition on flows of an Oldroyd 6-constant fluid,” *Journal of Computational and Applied Mathematics*, vol. 202, no. 2, pp. 402–413, 2007.

[30] R. I. Tanner, “Partial wall slip in polymer flow,” *Industrial and Engineering Chemistry Research*, vol. 33, no. 10, pp. 2434–2436, 1994.

[31] C. Le Roux, “Existence and uniqueness of the flow of second-grade fluids with slip boundary conditions,” *Archive for Rational Mechanics and Analysis*, vol. 148, no. 4, pp. 309–356, 1999.

[32] K. Vajravelu and A. Hadjinicolaou, “Convective heat transfer in an electrically conducting fluid at a stretching surface with uniform free stream,” *International Journal of Engineering Science*, vol. 35, no. 12-13, pp. 1237–1244, 1997.

[33] M. A. Delichatsios, “Air entrainment into buoyant jet flames and pool fires,” *Combustion and Flame*, vol. 70, no. 1, pp. 33–46, 1987.

[34] J. C. Crepeau and R. Clarksean, “Similarity solutions of natural convection with internal heat generation,” *Journal of Heat Transfer*, vol. 119, no. 1, pp. 183–185, 1997.

[35] R. C. Bataller, “Effects of heat source/sink, radiation and work done by deformation on flow and heat transfer of a viscoelastic fluid over a stretching sheet,” *Computers and Mathematics with Applications*, vol. 53, no. 2, pp. 305–316, 2007.

[36] G. Ahmadi, "Self-similar solution of incompressible micropolar boundary layer flow over asemi-infinite plate," *International Journal of Engineering Science*, vol. 14, pp. 639–646, 1976.

[37] K. A. Kline, "A spin-vorticity relation for unidirectional plane flows of micropolar fluids," *International Journal of Engineering Science*, vol. 15, no. 2, pp. 131–134, 1977.

[38] S. K. Jena and M. N. Mathur, "Similarity solutions for laminar free convection flow of a thermomicropolar fluid past a non-isothermal vertical flat plate," *International Journal of Engineering Science*, vol. 19, no. 11, pp. 1431–1439, 1981.

[39] J. Peddieson and R. P. Mcnitt, "Boundary layer theory for a micropolar fluid," *Recent Advances in Engineering Science*, vol. 5, pp. 405–426, 1970.

[40] S. E. El-Gendi, "Chebyshev solution of differential, integral and integro-differential equations," *Computer Journal*, vol. 12, pp. 282–287, 1969.

[41] Y. Morchoisn, "Pseudo-spectral space-time calculations of incompressible viscous flows," *AIAA Journal*, vol. 19, pp. 81–82, 1981.

[42] R. Nazar, A. Ishak, and I. Pop, "Unsteady boundary layer flow over a stretching sheet in a micropolar fluid," *International Journal of Mathematical, Physical and Engineering Sciences*, vol. 2, pp. 161–168, 2008.

[43] A. Ishak, "Thermal boundary layer flow over a stretching sheet in a micropolar fluid with radiation effect," *Meccanica*, vol. 45, pp. 367–373, 2010.

[44] L. J. Grubka and K. M. Bobba, "Heat transfer characteristics of a continuous stretching surface with variable temperature," *Journal of Heat Transfer*, vol. 107, no. 1, pp. 248–250, 1985.

[45] M. E. Ali, "Heat transfer characteristics of a continuous stretching surface," *Heat Mass Transfer*, vol. 29, no. 4, pp. 227–234, 1994.

[46] C.-H. Chen, "Laminar mixed convection adjacent to vertical, continuously stretching sheets," *Heat and Mass Transfer*, vol. 33, no. 5-6, pp. 471–476, 1998.